Chemical Science

ROYAL SOCIETY OF CHEMISTRY

EDGE ARTICLE

View Article Online
View Journal

Cite this: DOI: 10.1039/d5sc03783b

All publication charges for this article have been paid for by the Royal Society of Chemistry

Esterase-induced release of a theranostic prodrug in lysosomes for improved therapeutic efficacy and lower systemic toxicity

Sourav Dutta,†[a] Sanchita Tripathy, †[bc] Somnath Bej,†[a] Sabana Parvin,[a] Batakrishna Jana,*[ad] Chitta Ranjan Patra *[bc] and Amitava Das *[a]

Received 24th May 2025
Accepted 11th August 2025

DOI: 10.1039/d5sc03783b

rsc.li/chemical-science

5-Fluorouracil (5-FU) is the third most used chemotherapeutic agent. Despite being a frontline drug, it inhibits thymidylate synthase in malignant and non-malignant cells, which adds to its severe systemic toxicity. To address this, a new physiologically benign theranostic prodrug of 5-FU, named PD, has been developed by covalently linking 5-FU with a fluorophore and a lysosome-targeting morpholine moiety through an ester functionality. Esterase (Est), being overexpressed in various cancer cells such as human glioblastoma (U87) cells and human ovarian cancer (SKOV-3) cells, induces cleavage of the ester linkage and results in a sustained release of 5-fluorouracil-1-acetic acid (FUA), a precursor that liberates 5-FU in human physiology and subsequently 5-FU in lysosomes. The higher efficacy of PD in killing U87 (IC_{50}: ~20 μM for 48 h incubation) and SKOV-3 (with lower Est expression, IC_{50}: ~36 μM for 48 h incubation) cancer cell lines is attributed to the sustained and site-specific release of PD, with these values being much lower than the IC_{50} (≥50 μM) value for 5-FU in the U87 cell line. Importantly, the cell viability for PD, when used at a much higher concentration (50 μM) in normal Chinese Hamster Ovary (CHO) cells, was found to be ~95%, which confirms its potential efficacy in reducing systemic toxicity. The design of PD also enables us to achieve a 'TURN-ON' fluorescence response on Est-mediated cleavage of the ester functionality and demonstrates its potential for theranostic applications. Flow cytometry studies reveal death for live U87 cancer cells in both early and late apoptotic regions. CAM assay also confirmed the superiority of PD in limiting the development of the blood vasculature of the embryonic membrane to signify their antiangiogenic behaviour. The therapeutic efficacy of the PD is also demonstrated in a spheroid model, developed using human cervical cancer (HeLa) cell multicellular tumour sphere culture.

Introduction

5-Fluorouracil (5-FU), a pyrimidine analogue of the DNA/RNA base and an antimetabolite, is the third most widely used chemotherapeutic agent in the treatment of solid malignancies across the world.[1–4] The market size for 5-FU was valued at $2.45 billion in 2023, with an anticipated compound annual growth rate of 7.7% for the period 2024–2030.[5] However, 5-FU is also associated with severe cardiotoxicity, acute coronary syndrome, myocardial infarction, neurological abnormalities and severe toxicity, even causing death in patients having dihydropyrimidine dehydrogenase deficiency.[6,7] It also enhances the risk of infection due to compromised white blood cell counts. 5-FU has a narrow therapeutic index and is sparingly soluble in water. The plasma concentration of 5-FU is affected by numerous factors, thereby limiting its efficacy. A higher dose intensity of 5-FU is beneficial in improving the prognosis for treating gastrointestinal neoplasms—unfortunately, this also comes with dose-dependent toxicity.[8] It has been argued that efficacy could be improved through specific accumulation of 5-FU in the tumour-infected regions with sustained release.[9,10] Antibody–drug conjugates (ADCs) are one of the most popular choices for improving efficacy, as they allow site-specific drug release, improving effective local drug concentration at the tumour site, which helps in reducing drug doses and systemic toxicity of anticancer drugs.[11,12] An ADC of 5-FU is reported to preferentially target and inhibit HER2-expressing cancer cells. Research in ADCs is still in its infancy, and challenges like unfavourable pharmacokinetics, target-specific payload release, and off-target toxicity still limit the potential of different ADCs in clinical trials. Additionally, proteolytic cleavage could be an

[a]Department of Chemical Sciences, Centre for Advanced Functional Material, Indian Institute of Science Education and Research (IISER) Kolkata, Mohanpur, 741246, India. E-mail: amitava@iiserkol.ac.in

[b]Department of Applied Biology, CSIR-Indian Institute of Chemical Technology, Uppal Road, Tarnaka, Hyderabad – 500007, Telangana State, India. E-mail: crpatra@iict.res.in

[c]Academy of Scientific and Innovative Research (AcSIR), Ghaziabad-201002, India

[d]Department of Chemistry, School of Basic and Applied Sciences, Adamas University, Jagannathpur, Kolkata-700126, India. E-mail: batakrishna.jana1@adamasunivesrity.ac.in

† These authors contributed equally to this work.

immune evasion mechanism for ADCs.[13–15] To address this, fully human monoclonal antibodies (mAbs) have been used in recent ADCs. For most oncology mAbs, there is no clinically significant effect of binding or neutralising anti-drug antibodies in terms of pharmacokinetics.[16] Typically, non-human mAbs used in ADCs are large (~150 kDa), and this may limit their ability to penetrate target tissues and cells.[17,18] Very recently, Lan and coworkers have reported an ADC for 5-FU using a HER2-targeting protein, ZHER2:2891, fused with yeast cytosine deaminase (Fcy).[18] This needs extensive knowledge in designing/purifying his6-tagged Fcy fusion proteins and expertise in chemical biology involving time-consuming, intricate methodologies.

Despite several successes of clinically approved ADCs for therapeutic applications, certain factors pose challenges to their optimal use, such as metabolic instabilities toward proteolytic enzymes, rapid clearance, protein aggregation, or high aggregation propensity in the formulation and drug resistance mechanisms.[19–21] ADCs target overexpressed antigens at the surface of cancer cells, and tumour-specific antigens are limited in human physiology. Importantly, some of these antigens are endogenously expressed in other normal tissues. These, along with an unfavourable drug: payload distribution in ADCs, an insufficient target in heterogeneous tumours, and poor tissue penetration in solid tumours, contribute to a ≥1% accumulation of the dosed ADCs. This accounts for the undesired nonspecific release and off-target toxicity.[22] To evade these limitations, the concept of prodrugs has been introduced. Prodrugs are derivatives with favourable physicochemical and pharmacokinetic properties compared to the parent active pharmaceutical ingredient (API) and undergo biochemical transformation within the human physiology in the presence of endogenous stimuli/stimulus to generate the API *in situ* to initiate the desired pharmacological effect.[23–28] Prodrugs with improved absorption, distribution, metabolism, and excretion (ADME) properties are safer and more efficacious alternatives to parent drug molecules. Further, the prodrug concept utilises the 505(b)(2) pathway to save significant time and expenses when an FDA-approved drug is being used for prodrug development.[29,30] Thus, such a strategy is beneficial from a regulatory standpoint as well. Notably, approximately 13% of the drugs approved by the U.S. Food and Drug Administration (FDA) between 2012 and 2022 were prodrugs.[29–31]

Barring one report on an ADC of 5-FU, there is no example in the contemporary literature to address the issue of the high systemic toxicity of one of the most prescribed chemotherapeutic drugs.[32] Meanwhile, there are several literature reports on using 5-FU as a potential active API, and it is proposed that 5-FU induces cell cycle arrest at the S phase and causes cell death primarily through apoptosis.[33] The most crucial requirement for creating a prodrug system is site-specific delivery of the drug.[34,35] Delivering the prodrug directly into certain organelles enables the drug to be accumulated at its intended location (the subcellular compartment), thereby minimising drug efflux and decreasing the likelihood of side effects, representing a promising approach for effective cancer treatment.[36–39] Inspired by this, we have reported a lysosome-targeted prodrug (PD) derived from 5-fluorouracil-1-acetic acid (FUA) for targeted cancer therapy (Scheme 1a–c). FUA is a derivative of 5-FU and is known to undergo a proteolytic degradation process in human blood plasma to yield 5-FU.[40] FUA is conjugated with a benzimidazole-based fragment as a luminescent marker and a morpholine moiety as a lysosome targeting fragment to synthesise PD. Importantly, our design allows the luminescent marker to remain in the 'OFF state' when conjugated with FUA. FUA is conjugated to the luminescent marker through an ester linkage that is susceptible to an enzymatic cleavage in the presence of esterase (Est), an enzyme that is typically overexpressed in various cancer cells such as glioblastoma (U87) cells, human ovarian cancer (SKOV-3) cells and human cervical cancer (HeLa) cells.[41–45] FUA is expected to be released inside the lysosome of the Est overexpressed cancer cells, along with morpholine conjugated benzimidazole (E), a derivative that exists in the luminescent 'ON state'. Thus, one would expect to monitor the luminescence ON response to probe the release/distribution of FUA in lysosomes of a cancer cell in the presence of endogenous stimuli like Est. FUA, as reported earlier, undergoes an enzymatic cleavage to release 5-FU, the active API.[40,46–48] Confocal Laser Scanning Microscopy (CLSM) shows a higher cellular internalisation of PD compared to FUA and significant co-localisation with lysosomes in the U87 cells. MTT assay studies reveal that such a site-specific drug release reduces the systemic toxicity of PD, apart from favouring crucial issues like sustained drug release and increased drug efficacy compared to 5-FU, FUA and the prodrug without a lysosome targeting unit (D), where FUA is conjugated with a benzimidazole-based fragment. Thus, PD demonstrates compliance with the 505(b)(2) regulatory pathway. PD is found to induce cell cycle arrest at the S phase and causes cell death primarily through apoptosis, having antiangiogenic behaviour and causes significant inhibition of the 3D spheroid growth of the HeLa cancer cells.

Results and discussion

The details of all synthetic methodologies adopted for the synthesis of PD, FUA, and all necessary intermediates are provided in the Experimental section of the SI. The prodrug, PD, and all other intermediate compounds isolated during the synthesis processes were appropriately characterised using various analytical and spectroscopic techniques such as ^{1}H-NMR, ^{13}C-NMR and ESI-MS (Fig. S1–S15). All characterisation data for these intermediates and the final compound PD are discussed in the SI section. Spectroscopic and analytical data ensured the desired purity of the PD and all isolated intermediates. After successful synthesis, we performed the UV and luminescence spectroscopic analysis for PD (Fig. 1) and C (Fig. S16) to check the absorption and emission spectral patterns of both the fluorophore and the prodrug. All the spectroscopic measurements are done in 1× PBS buffer solution (pH 7.4). The absorption spectra recorded for PD and compound C reveal a broad absorption maximum at ~372 nm (ε: 17 400 M^{-1} and 25 500 M^{-1}, respectively) in 1× aq. PBS buffer medium (Fig. S16a). The emission spectra for PD and

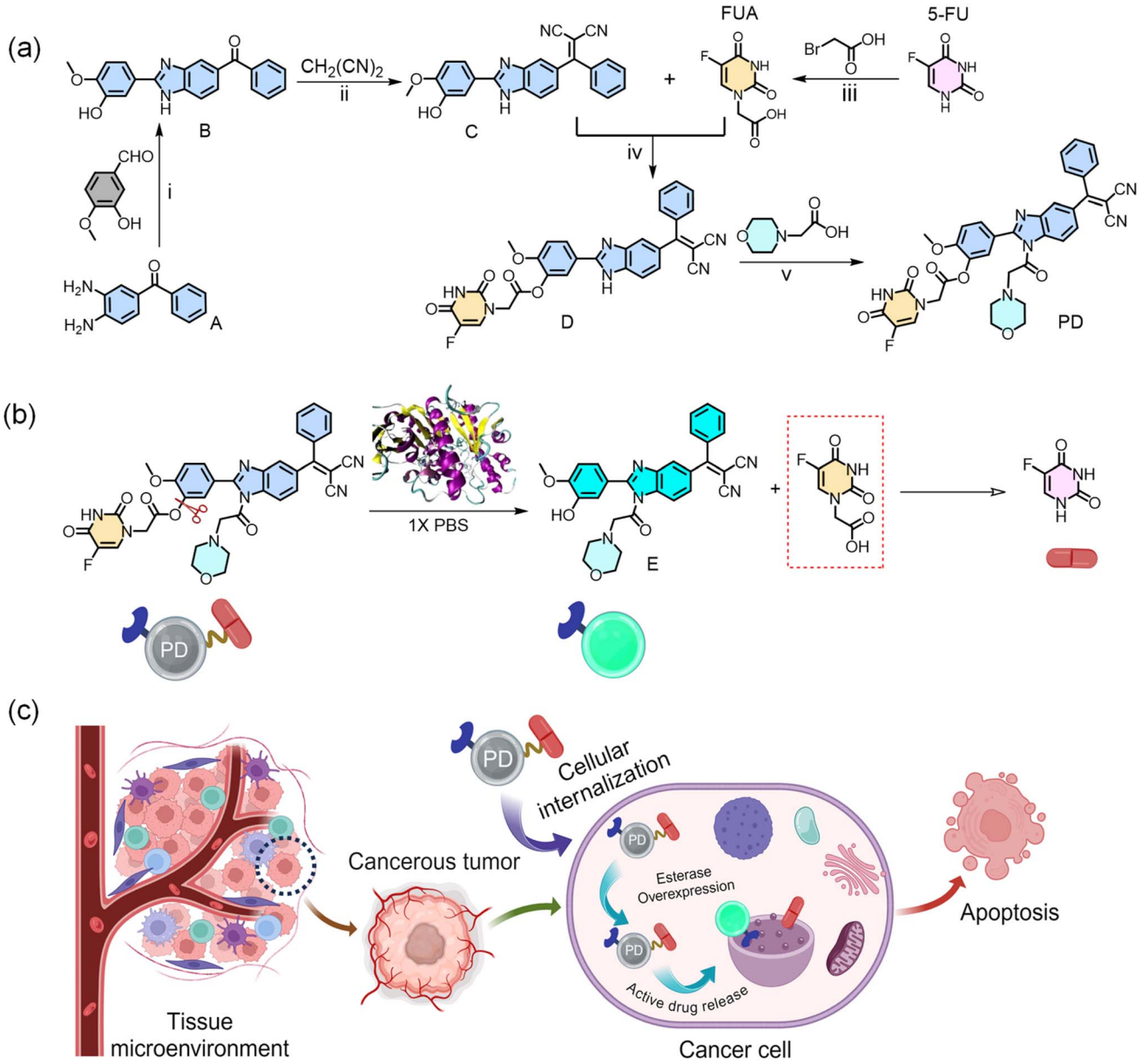

Scheme 1 (a) Molecular structures of 5-FU, FUA, PD, and all other intermediates used in synthesis and the synthetic scheme of PD: (i) $Na_2S_2O_5$, DMF, 100 °C; (ii) NH_4OAc, AcOH, toluene; (iii) KOH, water, 50 °C; (iv) EDC, HOBt, DMAP, DMF; (v) oxalyl chloride, dry DCM and then DIPEA, DMF, 0 °C. (b) Est-mediated drug release from PD. (c) Schematic representation of lysosome-targeted chemotherapeutic action and activation of PD inside the cancer cell (Created in BioRender. Sarkar, S. (2025) https://BioRender.com/5ids1f7).

compound C were recorded in 1× aq. PBS buffer following excitation at 373 nm, and an insignificant emission spectrum was observed for PD, while a broad emission band having $\lambda_{em}^{Max} \sim 430$ nm ($\lambda_{ext} = 373$ nm) was observed for C (Fig. S16b). Presumably, this is attributed to an interruption of the intramolecular CT process in PD due to the presence of the ester functionality. As a result, the fluorescence is in an 'OFF' state in PD. The ester functionality in PD is expected to undergo a cleavage reaction in the presence of the Est. To examine this, we further performed the electronic and luminescence spectroscopic studies of PD after incubation with Est. A detectable change in the absorption spectrum of the PD (10 μM, 1× PBS) was observed after incubation with 3 U per mL Est for 6 h (Fig. 1a, inset), while a new and broad emission band appeared at ~505 nm (Fig. 1a). Importantly, this emission spectrum of the cleaved product E after 6 h matched closely with the luminescence spectra for C (Scheme 1a), suggesting the effective cleavage of the ester functionality in PD induced by Est to yield E (Scheme 1b). Please note that both FUA, 5-FU and the morpholine moiety are non-luminescent. Intermediate compound D was also found to be practically non-luminescent as a result of interruption of the intramolecular CT process in D and PD due to the presence of the ester functionality (Fig. 1a). A plot of the change in luminescence intensity ($[F_t - F_0]$), where F_t and F_0 are

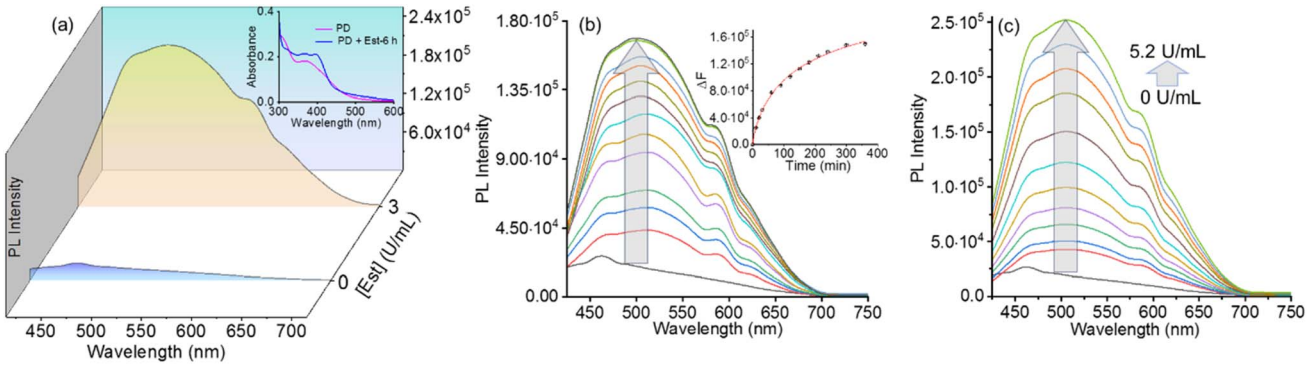

Fig. 1 (a) Emission spectra of PD (10 μM) in the absence and presence of the enzyme Est are recorded in phosphate buffer (pH 7.4), showing fluorescence activation upon Est treatment and absorption spectra in the inset. (b) The time-dependent release of E from PD upon Est treatment is recorded for 0, 0.5, 1, 1.5, 2, 2.5, 3, 3.5, 4, 5, and 6 h. The change in fluorescence intensity ΔF ($F_t - F_0$) as a function of time for 6 h is shown in the inset. (c) A consistent increase in fluorescence intensity in an Est concentration-dependent drug release study from 0 to 5.2 U mL^{-1} by starting the titration with 0.2 U mL^{-1} and then at a successive gap of 0.5 U mL^{-1}.

the luminescence intensities at time t and $t = 0$ respectively at 505 nm as a function of time revealed the cleavage of the ester functionality and the release of the E (Fig. 1b), which is also synonymous with the release of FUA reaching a plateau at ~6 h. To further corroborate our presumption, we performed luminescence studies using varying concentrations of Est (0 to 5.2 U mL^{-1}, with a successive increment of 0.5 U mL^{-1}, starting at 0.2 U mL^{-1}) in aqueous solution. PBS buffer medium (pH 7.4) was used to maintain a constant concentration of PD (10 μM) (Fig. 1c). A clear dependency of the generation of E as a function of [Est] also validated our proposition (Scheme 1b and Fig. 1c). This was reconfirmed by recording the fluorescence spectra of compound D in the presence of increasing concentrations of Est under analogous experimental conditions as in the case of PD. The observed enhancement in fluorescence intensity with rising Est levels further validates our proposition (Fig. S17). We also examined the role of pH in inducing the Est-mediated bond cleavages by monitoring the emission of fragment E (due to the Est-mediated cleavage of PD) and compound C at different media pH and maintaining other reaction conditions unchanged. A higher emission intensity for E at a lower pH suggests a more effective release of FUA at a lower pH (Fig. S18a and b). This also suggests a slow and sustained release of FUA and then 5-FU under physiological conditions (1× aq. PBS buffer, pH 7.4). Earlier reports suggest FUA undergoes intracellular metabolic transformation to yield 5-FU.[40,46–48] Higher glucose metabolism in cancer tissue/cells leads to enhanced H^+ production. Additionally, poor perfusion in malignant tumours results in an acidic extracellular pH (6.5–6.9) compared to normal tissue under physiological conditions (7.2–7.4).[49,50] Thus, the release of FUA from PD is expected to be further favoured in malignant tumours.

To confirm the specificity of this cleavage reaction towards Est, control experiments were performed by treating the 10 μM PD with 1 mM concentrations of various bioanalytes (Cys, Hcy, Arg, Trp, Asn, Met, Gly, Pro, His, GSH, Phe, Ile, Asp, Glu, Lys, Leu, Est). The absence of any detectable increase in luminescence intensity confirmed the specificity of the biochemical transformation involving PD and Est (Fig. S19). Further, the Est-induced release of FUA from PD was examined using reverse-phase high-performance liquid chromatography (RP-HPLC). RP-HPLC profiles for pre-synthesized and characterised PD, FUA, and intermediate C were recorded (Fig. 2). We used an analogous compound C as a reference to understand the possible retention time for E that was produced *in situ* from Est-treated PD. RP-HPLC was performed for 50 μM solutions of each of PD, FUA, C, and PD incubated with Est (5 U mL^{-1}) at different time intervals (2, 4, and 6 h) using acetonitrile/water (1 : 1) as eluent and performed isocratically. The detailed procedure and the experimental conditions are described in the SI. Retention times for different pre-synthesised species are as follows: t_{PD}: 5.93 min; t_{FUA}: 2.8 min; t_C: 6.98 min (Fig. 2). On incubation of PD with Est, two new peaks appeared with a retention time of 6.63 min and 2.8 min. Both peaks were found to increase with increasing incubation time (0–6 h). The new peak with a retention time of 6.63 min was relatively close to the retention time for C (t_C: 6.98 min) and was assigned to fragment E (Scheme 1b). The slightly lower retention time for E as compared to C can be rationalised based on the presence of a lysosome-targeting, more polar morpholine group in E. The other peak at 2.8 min appeared at the same place as for FUA and confirmed its release through the enzymatic cleavage of PD. Thus, RP-HPLC studies

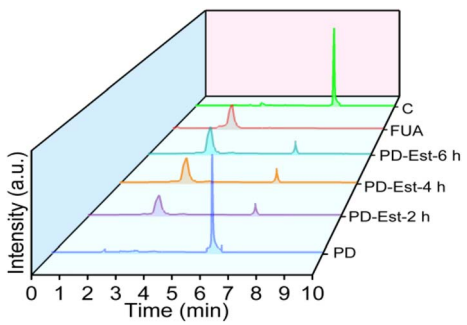

Fig. 2 RP-HPLC spectrum profile for PD, C, FUA, and Est-treated PD (50 μM each) after 2, 4, and 6 h in 1× PBS buffer solution.

confirmed the release of FUA and E on the enzymatic cleavage of PD induced by Est.

After ensuring the Est-mediated *in vitro* release of FUA, which undergoes further metabolic processes to release 5-FU at the cancer tissue/cells,[40,46–48] along with the lysosome-targeted luminescence marker E, we further examined the cellular internalisation of PD in the U87 cancer cell line using a CLSM (confocal laser scanning microscope). The overexpression of Est in cancer cell lines such as U87 is linked to increased cell proliferation and invasion.[51–53] The cellular uptake studies of the PD were carried out using U87 cell lines through CLSM (Fig. 3a–d). A green fluorescence was observed (indicated by a white arrow) in U87 cells, incubated with the PD for 24 h. This was rationalised as the intrinsic luminescence of fragment E, generated through enzymatic cleavage induced by endogenous Est overexpressed in tumour cells (Fig. 3d and S20a). Est activity in malignant colorectal tumours (0.45 ± 0.25 U L^{-1} for males and 0.45 ± 0.35 U L^{-1} for females) is much higher than in normal tissues (0.17 ± 0.09 U L^{-1} for males and 0.12 ± 0.07 U L^{-1} for females).[54] Reports suggest that stored fats in malignant tumours are released and support Est-induced cancer pathogenesis.[55,56] We have earlier established that the release of E is also associated with the release of an equimolar amount of FUA. Incubation with either FUA or C, used at identical concentrations to PD, failed to show any similar uptake (Fig. 3b and c). The confocal microscopic images are quantified using IMAGEJ software and presented in Fig. S20b, which also supports the above results. The terminal-COOH functionality in FUA remains as a carboxylate and fails to diffuse through the lipid core of the plasma membrane. This accounts for a lower cell membrane permeability and reported cytotoxicity of FUA toward different cancer cells (A431, HT29, and HeLa cells) compared to 5-FU.[57–59] Thus, the ester functionality in PD, as evident in CLSM images (Fig. 3d), helps in improving the cellular permeabilisation of FUA.

Following this, we checked for colocalization of PD in mitochondria/lysosomes using mito-tracker red/lyso-tracker red through CLSM studies. The U87 cells were treated with FUA, C, and PD for 24 h, followed by incubation with mito-/lyso-tracker red for 15–20 min before the termination of the experiment to stain the subcellular organelles, mitochondria/lysosomes. Results of the intracellular co-localisation of PD with U87 cells are presented in Fig. S21 and 4a–c. Results reveal that when U87 cells are incubated with PD, individual green and red fluorescence (for *in situ* release of E) was observed in the FITC (for uptake of the prodrug molecule) and Cy5 channels (for

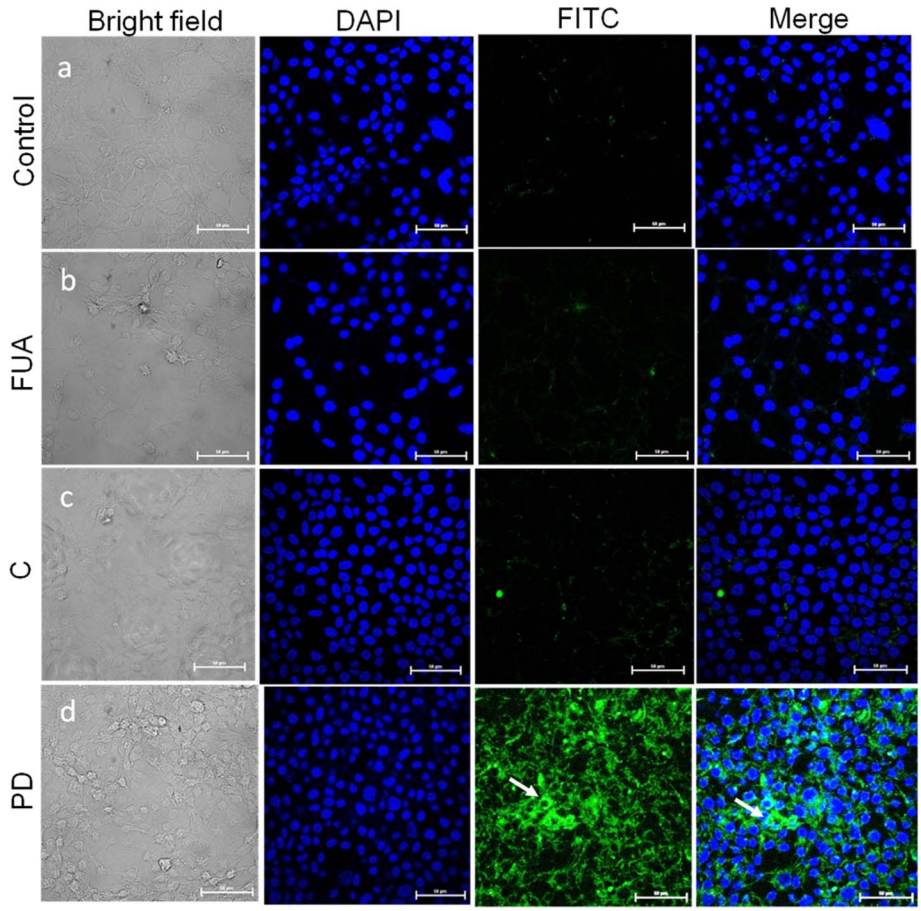

Fig. 3 Representative images of cellular uptake of our designed prodrug and respective control molecules in U87 cells: (a) control, (b) FUA (10 μM), (c) C (10 μM), and (d) PD (10 μM); where Column I: bright field, II: DAPI, III: FITC, IV: merged images. The images were acquired using confocal microscopy (laser used DAPI: 404.2, PD/C/FUA: 535 nm, green) at 60× magnification, scale bar = 50 μm.

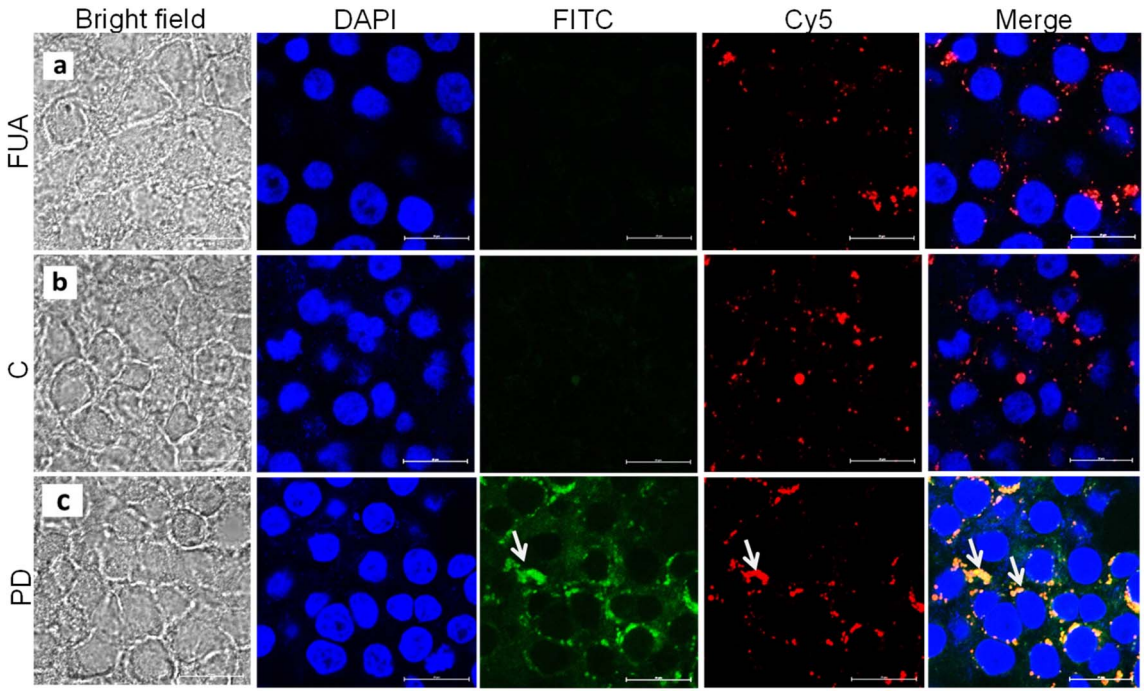

Fig. 4 Representative images of lysosomal internalisation of our designed prodrug (PD) and respective control molecules (FUA and C) in U87 cells using lyso-tracker red: (a) FUA (10 μM), (b) C (10 μM), and (c) PD (10 μM); where Column I: bright field, II: DAPI, III: FITC, IV: Cy5, V: merged images. The images were acquired in confocal microscopy (laser used for DAPI: 404.2 nm, PD/FUA/C: 535 nm (green), and lysotracker: 595 nm (red) at 60× magnification), scale bar = 50 μm.

mitochondria/lysosome staining), respectively. The green fluorescence in the FITC channel further confirms the release of FUA and eventually 5-FU in malignant tumours through the enzymatic cleavage of the ester functionality in PD by endogenous Est. The merged image of the FITC channel with Cy5 indicates that PD molecules, even though internalised into the cell, are not localised in the subcellular organelle mitochondria (individual green and red fluorescence: Fig. S21c), but they are localised in the lysosome (yellow fluorescence due to merging of red & green: Fig. 4c). Thus, CLSM images of the colocalization studies with lysotracker red/mitotracker red confirm that the release of E happens in lysosomes, not in mitochondria. The localisation of E in the lysosome also ensures the localisation of PD in the lysosome. Lysosomes typically maintain a highly acidic environment (pH ∼ 4.5–5.0), which favours the localisation of the morpholine functionality present in E and PD. Also, no fluorescence within the lysosome was observed for other control molecules, FUA and C (Fig. 4a and b). This confirmed the design philosophy for developing the purpose-built prodrug PD and its effective release in the lysosome for better therapeutic efficacy.

We further examined the cell viability of FUA, 5-FU, PD, and C towards various cancer cell lines (U87, SKOV-3) using MTT assay in a dose-dependent (1–100 μM) and time dependent (48 h and 72 h) manner, and compared the cytotoxicity results with normal Chinese Hamster Ovary (CHO) cell lines. It is evident from Fig. S22 that CHO cells, incubated with PD/FUA/C, show insignificant toxicity after 48 h incubation even at a higher concentration (50 μM). Further, the cytotoxic properties of PD, FUA, 5-FU and C were evaluated in different cancer cell lines (U87 and SKOV-3; Fig. 5a–d) following incubation over varying time. Results revealed that PD adversely affected the cancer cell viability in a dose (1–100 μM) and time-dependent manner (48 and 72 h) and was more cytotoxic towards cancer cell lines as compared to other precursor compounds (FUA and C). Even the actual drug 5-FU shows lesser toxicity as compared to PD. Table S1 summarises the IC_{50} value of PD and other control molecules in U87 and SKOV-3 cell lines. Importantly, PD induced higher toxicity towards U87 cell lines at lower concentrations, with an IC_{50} value of 20.77 and 16.95 μM on incubation for 48 and 72 h, respectively. The IC_{50} values of PD in SKOV-3 cells were found to be 36.85 and 32.47 μM, respectively, on incubation for 48 and 72 h. Also, PD is found to be more toxic than naked 5-FU, which shows higher toxicity than FUA but less toxicity than PD in both U87 and SKOV-3 cell lines. To further investigate the lysosome-targeting effect, we evaluated the cytotoxicity of compound D in U87 cancer cells and CHO normal cells over a 48 h incubation period. Compound D exhibited negligible toxicity toward CHO cells at concentrations up to 50 μM, while demonstrating a moderate cytotoxic effect in U87 cells, with an IC_{50} value of 80.5 μM after 48 h of treatment (Fig. S22 and S23). These studies confirmed that PD is also more toxic than D, and this essentially confirms the role of lysosome-specificity of PD as compared to D. This demonstrates the importance of the specificity of PD towards lysosomes, which subsequently causes higher toxicity owing to a higher local concentration of PD inside the cancer cell organelle. Since PD is more cytotoxic towards U87 cell lines, other *in vitro* experiments are carried out in this cell line using

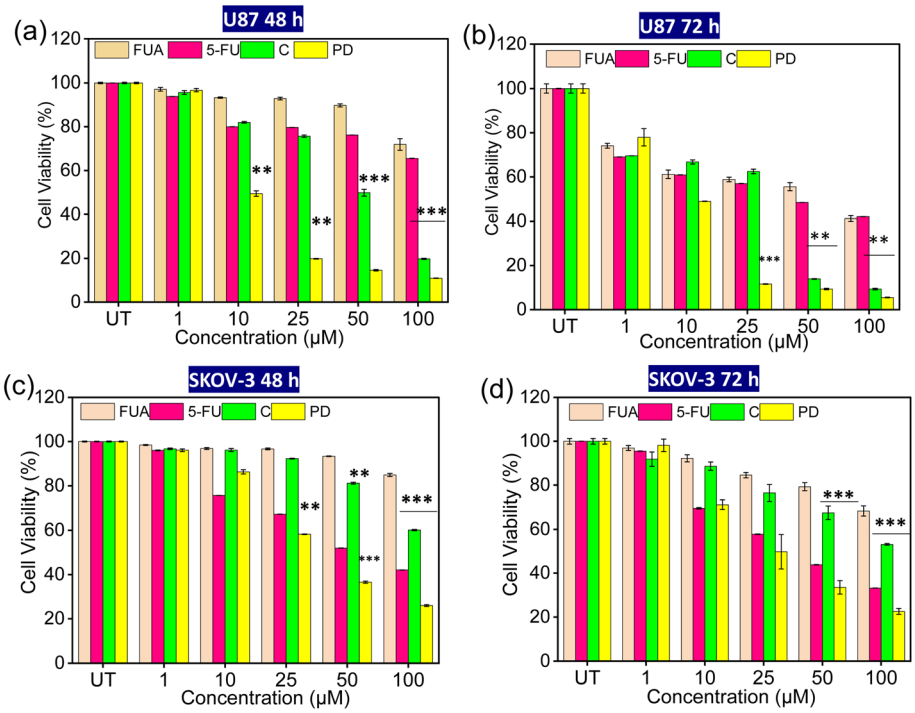

Fig. 5 Cell viability assay in several cancer cell lines, such as (a and b) U87 and (c and d) SKOV-3. Our designed prodrug and respective control molecules (PD, FUA, 5-FU, and C) show a decrease in the cancer cell viability in a dose (1–100 μM) and time (48 and 72 h) dependent manner. These experiments were performed in triplicate and represented as mean ± SD. Significant differences from untreated cells were observed at (*p < 0.05, **p < 0.01, ***p < 0.001).

a 10 μM concentration (lower than the IC_{50} value). Presumably, a higher expression of Est enzymes in the U87 cell line compared to other cell lines accounts for the higher toxicity of PD.[41,42] The observed toxicity of PD towards U87 cells further corroborates the observations of earlier researchers that FUA undergoes intracellular biochemical transformation to generate 5-FU.[40,46–48]

An anticancer drug can inhibit cancer cell proliferation at different phases (sub-G1, G0–G1, S, and G2/M). To check the arrested phase in U87 cells in response to FUA, C, and PD (10 μM each), cell cycle analyses were carried out using flow cytometry after staining the cells with a PI mix (Fig. 6a(i–v)). Several reports demonstrate that 5-FU arrests the cancer cell proliferation primarily at the S phase, apart from the G2/M phase.[32] For PD, cell cycle arrest for U87 cells happens at the S phase and also to some extent in the G2/M phase, potentiating their cell death-inducing property (Fig. 6a(iv)). However, for FUA and C, no significant cell cycle arrest (Fig. 6a(i–iii)) was observed. The % of cell populations for all flow cytometry data was analysed and is presented in Fig. 6a(v).

The cell death process was studied using FACS (Fluorescence-Activated Cell Sorting) studies to understand the programmed cell death-inducing potential of PD toward U87 cell lines (Fig. 6b(i–v)). For this, U87 cells were incubated with annexin V/FITC and PI, and the % of cells in different phases was investigated through flow cytometry. In the early phases of apoptosis, annexin V preferentially binds to phosphatidylserine that is visible on the plasma membrane's outer leaflet. On the other hand, PI is a DNA intercalating agent that penetrates late apoptotic and necrotic cells but is excluded from viable cells with intact membranes. Q1 (FITC−/PI+), Q2 (FITC+/PI+), Q3 (FITC−/PI−), and Q4 (FITC+/PI−) quadrants represent necrotic, late apoptotic, healthy and early apoptotic cell populations, respectively. Results reveal that, in response to PD, the % of the U87 cell population is higher in both early and late apoptotic regions as compared to other precursor molecules (FUA and C) and the untreated control group, which is also supported by an earlier report.[60] Percentage (%) of the cell population at different phases was also analysed and graphically presented in Fig. 6b(v). The results altogether indicate the apoptosis-inducing properties of PD molecules towards U87 cells.

We further performed a chick embryo chorioallantoic membrane (CAM) assay to check the antiangiogenic properties of PD. CAM possesses an extensive capillary network expressing fibroblast growth factor 2 that limits the development of the vascular system of the embryonic membrane.[61,62] CAM assay is a simple *in vivo* model to study the effect of new drugs on the extraembryonic membrane of the developing chick embryo. We performed the CAM assay to study the effect of PD, C, and FUA on the extraembryonic membrane of developing chick embryos. The results are presented in Fig. 7. A narrow hole was created on the fertilized eggs on day 4 and the chorioallantoic membrane was incubated with our designed prodrug (PD) and respective control molecules (FUA and C) at 100 μM each for 4 h. Results revealed that there was a slight disruption of blood vasculature upon FUA and C incubation. However, a significant inhibition of blood vasculature was observed when the chorioallantoic membrane was incubated with the prodrug molecules (PD)

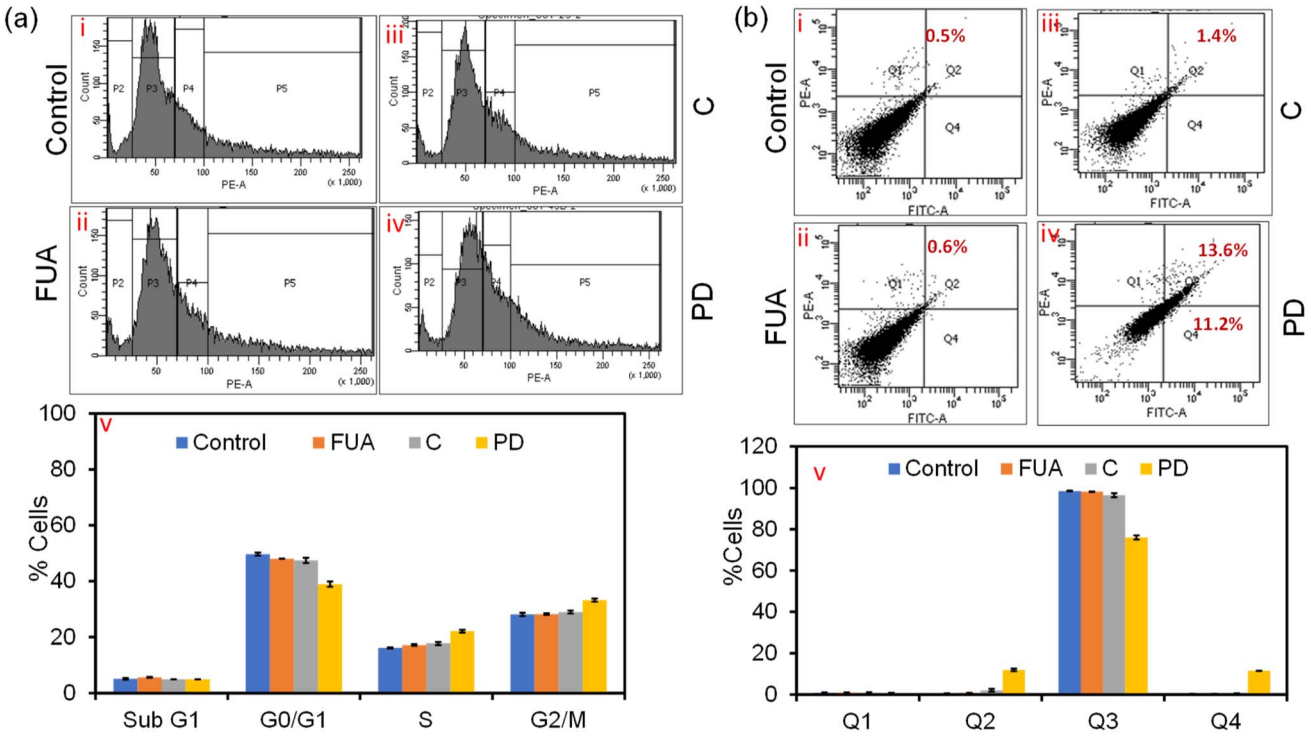

Fig. 6 Cell cycle and apoptosis analyses in U87 cells: in Panel I (cell cycle analysis): (a) (i) control, (ii) FUA, (iii) C, (iv) PD, and (v) graphical representation of % cells in different phases of the cell cycle. The prodrug molecule PD arrests the U87 cells in the S and G2/M phases. Panel II (apoptosis analysis): (b) (i) control, (ii) FUA, (iii) C, (iv) PD, and (v) graphical representation of % cells in different apoptotic phases. The prodrug molecule PD exhibits both early and late apoptotic cell death. Three independent experiments were performed and represented as mean ± SD.

exhibiting their antiangiogenic properties. The blood vessel diameter was quantified to reveal the % of fold change using ImageJ software and presented in Fig. S24 & Table S2, which also matched well with the above observation. This further confirmed the efficacy of PD as a stimulus-responsive organelle-specific anti-cancer drug.

Finally, we have investigated the effectiveness of PD and FUA in 3D multicellular tumour spheroids. HeLa cell multicellular tumour sphere culture (MCTS) in three dimensions was developed in our lab following the previously described 3D sphere creation for tumour mimicking.[63] Spheroid models are considered a close representation of *in vivo* models.[64] A significant decrease in the size of the spheroids was observed for the PD (50 μM) treated group compared to the group treated with FUA (50 μM; Fig. 8). An increase in the size of the spheroids was observed in the control group. This data further validates the

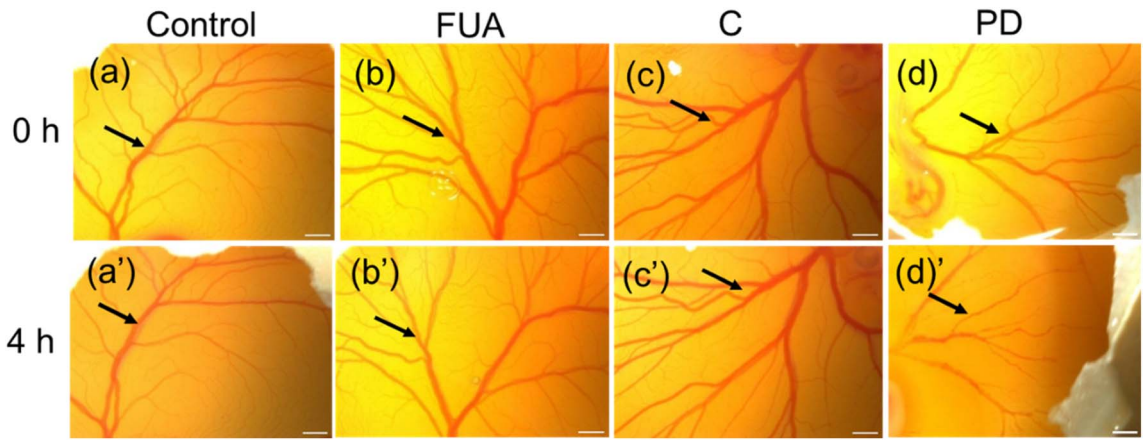

Fig. 7 Chorioallantoic membrane assay. Representative CAM images at 0 and 4 h: (a and a′) control, (b and b′) FUA, (c and c′) C, and (d and d′) PD. The blood vessels of the chick embryo are more inhibited in response to the PD molecules (indicated by black arrows), potentiating the anti-angiogenic potential of the pro-drug molecules. Images were taken using a Leica stereo microscope at 1× magnification, scale bar = 5 mm.

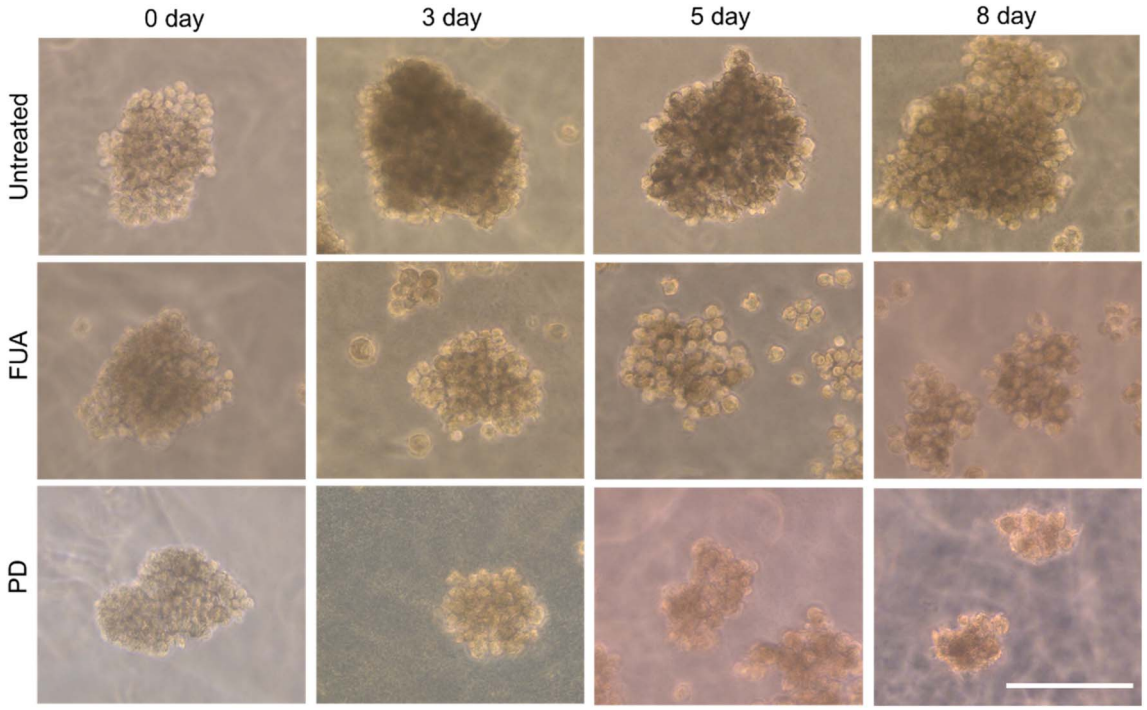

Fig. 8 Bright field images indicating the size of the spheroid on the indicated day after FUA and PD treatment, along with the control. The size is significantly decreased in both the FUA and PD-treated groups, and PD has better efficacy compared to FUA. The scale bar corresponds to 100 μm.

higher efficacy of the PD compared to that of FUA in inhibiting spheroid growth, which closely mimics the main features of human solid tumours.

Conclusion

5-FU is an anti-metabolite that interferes with the synthesis and function of DNA and RNA in cancer cells by inhibiting thymidylate synthase in malignant and non-malignant cells, which induces severe systemic toxicity. A new lysosome-targeted prodrug (PD) is synthesised to address the issue of high systemic toxicity by enhancing the efficacy through sustained release of 5-FU specifically in lysosomes through functionalization with morpholine. Further, it is demonstrated that by leveraging the overexpression of Est enzymes in human glioblastoma (U87) cells, site-specific, sustained, and sequential release of the FUA and 5-FU in the lysosome is achieved. It is not unreasonable to link these to the higher efficacy of PD in killing U87 and SKOV-3 cancer cell lines. The design of PD enabled us to realise a 'TURN-ON' fluorescence response upon Est-mediated cleavage of the ester functionality and confirmed its potential for theranostic applications.[65] IC_{50} values for PD for U87 and SKOV-3 cells are found to be 20.77 and 36.85 μM, respectively, on incubation for 48 h. Meanwhile, the IC_{50} values for 5-FU in U87 and SKOV-3 cells are ∼105 and 48 μM, respectively, under identical experimental conditions. Importantly, the cell viability for PD, when used at a much higher concentration (50 μM) in normal healthy CHO cells, is found to be ∼95%, which confirms its potential efficacy in reducing systemic toxicity. Flow cytometry studies in U87 cells confirm that PD causes both early and late apoptotic death as compared to other precursor molecules (FUA and C) and the untreated control group. Importantly, the CAM assay confirmed the superiority of PD in limiting the development of the blood vasculature of the embryonic membrane to signify its antiangiogenic behaviour. Efficacy is also demonstrated in a 3D spheroid model developed using HeLa cell multicellular tumour sphere culture. A significant decrease in the size of the spheroids was observed for the PD (50 μM) treated group compared to the group treated with FUA (50 μM).

Author contributions

Sourav Dutta: scholar associated with the synthesis, scale up synthesis, characterization, photochemical and physicochemical studies, and manuscript preparation. Sanchita Tripathy: scholar associated with *in vitro* cell culture and angiogenesis studies, manuscript preparation. Somnath Bej: associated with synthesis, design and photochemical studies. Sabana Parvin: associated partly with synthesis and characterization. Batakrishna Jana: biological studies, interpretation and correlation of the data, and writing of this article. Chitta Ranjan Patra: overall supervision of intracellular and angiogenesis studies, interpretation and correlation of the biological data and writing of this article. Amitava Das: conceptualization, overall supervision, interpretation and data correlation, overall coordination, and writing of the article.

Conflicts of interest

The authors declare no conflicts of interest.

Data availability

The data supporting this article have been included as part of the SI. See DOI: https://doi.org/10.1039/d5sc03783b.

Acknowledgements

A. D. acknowledges the ANRF-J.C. Bose Fellowship and funding through the JBR/2023/000005 grant. A. D. also acknowledges the MoE-STARS research grant (No. 2023-47) for financial support. S. D. acknowledges IISER Kolkata for the Senior Research Fellowship (SRF). S. B. acknowledges the ANRF Postdoctoral Fellowship award (PDF/2023/003483) for financial support. B. J. acknowledges the ANRF-Ramanujan Fellowship (RJF/2022/000127) for support. C. R. P. is thankful to DST, New Delhi (CRG/2022/004594: GAP0985) for financial support for this research. S. T. is grateful to UGC for her Research Fellowship. The authors acknowledge the Central Instrumentation Facility (iCIF) of IISER Kolkata. C. R. P. and S. T. thank the Director, CSIR-IICT (Ms. No. IICT/Pubs./2025/177 dated May 13, 2025) for providing all the required facilities to carry out the work.

References

1 J. D. Sara, J. Kaur, R. Khodadadi, M. Rehman, R. Lobo, S. Chakrabarti, J. Herrmann, A. Lerman and A. Grothey, *Ther. Adv. Med. Oncol.*, 2018, **10**, 1–18.
2 D. B. Longley, D. P. Harkin and P. G. Johnston, *Nat. Rev. Cancer*, 2003, **3**, 330–338.
3 K. Miura, M. Kinouchi, K. Ishida, W. Fujibuchi, T. Naitoh, H. Ogawa, T. Ando, N. Yazaki, K. Watanabe, S. Haneda, C. Shibata and I. Sasaki, *Cancers*, 2010, **2**, 1717–1730.
4 J.-K. Chen, K. A. Merrick, Y. W. Kong, A. I. Tomasevic, G. Eng, E. D. Handly, J. C. Patterson, I. G. Cannell, L. S. Lopez, A. M. Hosios, A. Dinh, D. S. Kirkpatrick, K. Yu, C. M. Rose, J. M. Hernandez, H. Hwangbo, A. C. Palmer, M. G. V. Heiden, Ö. H. Yilmaz and M. B. Yaffe, *Cell Rep. Med.*, 2024, **5**, 101778.
5 *Global Fluorouracil (5FU) Market Size By Type, By Route of Administration, By Geographic Scope And Forecast*, https://www.verifiedmarketresearch.com/product/fluorouracil-5fu-market/#:~:text=Fluorouracil(5FU)Marketwasvalued,7.7%25from2024to2030, accessed 20 May 2025.
6 C. Yuan, H. Parekh, C. Allegra, T. J. George and J. S. Starr, *Cardio-Oncology*, 2019, **5**, 13.
7 J. Latchman, A. Guastella and C. Tofthagen, *Clin. J. Oncol. Nurs.*, 2014, **18**, 581–585.
8 J. J. Lee, J. H. Beumer and E. Chu, *Cancer Chemother. Pharmacol.*, 2016, **78**, 447–464.
9 G. Huang, Y. Xie, Z. Jiang, Z. Xu, Z. Jin and K. Xu, *Curr. Probl. Surg.*, 2025, **66**, 101746.
10 P. M. Wallace, J. F. MacMaster, V. F. Smith, D. E. Kerr, P. D. Senter and W. L. Cosand, *Cancer Res.*, 1994, **54**, 2719–2723.
11 A. Thomas, B. A. Teicher and R. Hassan, *Lancet Oncol.*, 2016, **17**, e254–e262.
12 Z. Fu, S. Li, S. Han, C. Shi and Y. Zhang, *Signal Transduction Targeted Ther.*, 2022, **7**, 93.
13 T. Miyoshi-Akiyama, I. Ishida, M. Fukushi, K. Yamaguchi, Y. Matsuoka, T. Ishihara, M. Tsukahara, S. Hatakeyama, N. Itoh, A. Morisawa, Y. Yoshinaka, N. Yamamoto, Z. Lianfeng, Q. Chuan, T. Kirikae and T. Sasazuki, *J. Infect. Dis.*, 2011, **203**, 1574–1581.
14 M. G. Romei, B. Leonard, I. Kim, H. S. Kim and G. A. Lazar, *J. Biol. Chem.*, 2023, **299**, 104685.
15 D. M. H. Van Rijswijck, A. Bondt, N. De Kat, R. Lood and A. J. R. Heck, *Anal. Chem.*, 2024, **96**, 23–27.
16 M. Grairi and M. L. Borgne, *Drug Discovery Today*, 2024, **29**, 104241.
17 Global Antibody-drug Conjugates Market, Strategic Market Research Website, https://www.strategicmarketresearch.com/market-report/antibody-drugconjugates-market, published June 2022, accessed 10 October 2024.
18 K.-H. Lan, C.-L. Tsai, Y.-Y. Chen, T.-L. Lee, C.-W. Pai, Y. Chao and K.-L. Lan, *Biochem. Biophys. Res. Commun.*, 2021, **582**, 137–143.
19 C. McKertish and V. Kayser, *Biomedicines*, 2021, **9**, 872.
20 K. Tsuchikama and Z. An, *Protein Cell*, 2018, **9**, 33–46.
21 H. Gao, Z. Xi, J. Dai, J. Xue, X. Guan, L. Zhao, Z. Chen and F. Xing, *Mol. Cancer*, 2024, **23**, 88.
22 H. E. Marei, C. Cenciarelli and A. Hasan, *Cancer Cell Int.*, 2022, **22**, 255.
23 Y. Wang, D. Xiao, J. Li, S. Fan, F. Xie, W. Zhong, X. Zhou and S. Li, *Signal Transduction Targeted Ther.*, 2022, **7**, 20.
24 J. B. Zawilska, J. Wojcieszak and A. B. Olejniczak, *Pharmacol. Rep.*, 2013, **65**, 1–14.
25 M. Markovic, S. Ben-Shabat and A. Dahan, *Pharmaceutics*, 2020, **12**, 1031.
26 X. Xie, T. Yu, X. Li, N. Zhang, L. J. Foster, C. Peng, W. Huang and G. He, *Signal Transduction Targeted Ther.*, 2023, **8**, 335.
27 A. Husain, J. Monga, S. Narwal, G. Singh, M. Rashid, O. Afzal, A. Alatawi and N. M. Almadani, *Chem. Biodiversity*, 2023, **20**, e202301169.
28 M. A. M. Subbaiah, J. Rautio and N. A. Meanwell, *Chem. Soc. Rev.*, 2024, **53**, 2099–2210.
29 W. F. Salminen, O. Aloba, A. Drew, A. Marcinowicz and M. Huang, *Drug Discovery Today*, 2023, **28**, 103618.
30 W. F. Salminen, M. E. Wiles and R. E. Stevens, *Drug Discovery Today*, 2019, **24**, 46–56.
31 M. M. De Souza, A. L. R. Gini, J. A. Moura, C. B. Scarim, C. M. Chin and J. L. Dos Santos, *Pharmaceuticals*, 2025, **18**, 297.
32 P. M. De Angelis, D. H. Svendsrud, K. L. Kravik and T. Stokke, *Mol. Cancer*, 2006, **5**, 20.
33 J. Rautio, N. A. Meanwell, L. Di and M. J. Hageman, *Nat. Rev. Drug Discovery*, 2018, **17**, 559–587.

34 R. Tiwari, P. S. Shinde, S. Sreedharan, A. K. Dey, K. A. Vallis, S. B. Mhaske, S. K. Pramanik and A. Das, *Chem. Sci.*, 2021, **12**, 2667–2673.
35 W. Chen, G. Luo and X. Zhang, *Adv. Mater.*, 2019, **31**, 1802725.
36 S. Pal, V. Ramu, N. Taye, D. Mogare, A. Yeware, D. Sarkar, D. S. Reddy, S. Chattopadhyay and A. Das, *Bioconjugate Chem.*, 2016, **27**, 2062–2070.
37 S. Sarkar, A. Chatterjee, D. Kim, C. Saritha, S. Barman, B. Jana, J.-H. Ryu and A. Das, *Adv. Healthcare Mater.*, 2024, **6**, e2403243.
38 B. Jana, S. Jin, E. M. Go, Y. Cho, D. Kim, S. Kim, S. K. Kwak and J.-H. Ryu, *J. Am. Chem. Soc.*, 2023, **145**, 18414–18431.
39 L. Yang, R. Peltier, M. Zhang, D. Song, H. Huang, G. Chen, Y. Chen, F. Zhou, Q. Hao, L. Bian, M.-L. He, Z. Wang, Y. Hu and H. Sun, *J. Am. Chem. Soc.*, 2020, **142**, 18150–18159.
40 Q. Luo, P. Wang, Y. Miao, H. He and X. Tang, *Carbohydr. Polym.*, 2012, **87**, 2642–2647.
41 Z. Ye, L. Gao, J. Y. Cai, Y. X. Wang, Y. Li, S. A. Tong, T. F. Yan, Q. Sun, Y. Z. Qi, Y. Xu, H. Jiang, S. Zhang, L. Zhao, S. Zhang and Q. Chen, *Nanomed. Nanotechnol. Biol. Med.*, 2022, **44**, 102581.
42 Y. Y. Ma, W. J. Gao, S. H. Ma, Y. Y. Liu and W. Y. Lin, *Anal. Chem.*, 2020, **92**, 13405–13410.
43 N. Qiu, X. Liu, Y. Zhong, Z. Zhou, Y. Piao, L. Miao, Q. Zhang, J. Tang, L. Huang and Y. Shen, *Adv. Mater.*, 2016, **28**, 10613–10622.
44 Z. Zhou, W. J. Murdoch and Y. Shen, *J. Polym. Sci., Part A: Polym. Chem.*, 2016, **54**, 507–515.
45 Y. Z. Yang, Z. Y. Xu, N. B. Li and H. Q. Luo, *Spectrochim. Acta, Part A*, 2021, **262**, 120094.
46 Y. Sun, J. A. Kaplan, A. Shieh, H.-L. Sun, C. M. Croce, M. W. Grinstaff and J. R. Parquette, *Chem. Commun.*, 2016, **52**, 5254–5257.
47 V. Ciaffaglione, M. N. Modica, V. Pittalà, G. Romeo, L. Salerno and S. Intagliata, *ChemMedChem*, 2021, **16**, 3496–3512.
48 P. Chakraborty and P. Dastidar, *Chem. Commun.*, 2019, **55**, 7683–7686.
49 V. Estrella, T. Chen, M. Lloyd, J. Wojtkowiak, H. H. Cornnell, A. Ibrahim-Hashim, K. Bailey, Y. Balagurunathan, J. M. Rothberg, B. F. Sloane, J. Johnson, R. A. Gatenby and R. J. Gillies, *Cancer Res.*, 2013, **73**, 1524–1535.
50 I. Böhme and A. K. Bosserhoff, *Pigm. Cell Melanoma Res.*, 2016, **29**, 508–523.
51 B. Nowak, P. Rogujski, M. Janowski, B. Lukomska and A. Andrzejewska, *Biochim. Biophys. Acta, Rev. Cancer*, 2021, **1876**, 188582.
52 A. Wlodarczyk, D. Grot, E. Stoczynska-Fidelus and P. Rieske, *J. Oncol.*, 2020, **2020**, 6783627.
53 A. K. Madikonda, A. Ajayakumar, S. Nadendla, J. Banothu and V. Muripiti, *Bioorg. Med. Chem.*, 2024, **116**, 118001.
54 H. Dong, L. Pang, H. Cong, Y. Shen and B. Yu, *Drug Delivery*, 2019, **26**, 416–432.
55 H. Qin and Z.-H. Ruan, *Cell Biochem. Biophys.*, 2014, **70**, 33–36.
56 D. K. Nomura, J. Z. Long, S. Niessen, H. S. Hoover, S.-W. Ng and B. F. Cravatt, *Cell*, 2010, **140**, 49–61.
57 B. K. Gan, K. Rullah, C. Y. Yong, K. L. Ho, A. R. Omar, N. B. Alitheen and W. S. Tan, *Sci. Rep.*, 2020, **10**, 16867.
58 R. M. Wohlhueter, R. S. McIvor and P. G. Plagemann, *J. Cell. Physiol.*, 1980, **104**, 309–319.
59 Sauraj, S. U. Kumar, P. Gopinath and Y. S. Negi, *Carbohydr. Polym.*, 2017, **157**, 1442–1450.
60 U. Fischer, S. Steffens, S. Frank, N. G. Rainov, K. Schulze-Osthoff and C. M. Kramm, *Oncogene*, 2005, **24**, 1231–1243.
61 S. Javerzat, P. Auguste and A. Bikfalvi, *Trends Mol. Med.*, 2002, **8**, 483–489.
62 T. Jia, T. Jacquet, F. Dalonneau, P. Coudert, E. Vaganay, C. E. Héritier, J. Vollaire, V. Josserand, F. Ruggiero, J.-L. Coll and B. Eymin, *BMC Biol.*, 2021, **19**, 173.
63 L. Wang, H. Guo, C. Lin, L. Yang and X. Wang, *Mol. Med. Rep.*, 2014, **9**, 2117–2123.
64 A. S. Nunes, A. S. Barros, E. C. Costa, A. F. Moreira and I. J. Correia, *Biotechnol. Bioeng.*, 2019, **116**, 206–226.
65 S. K. Pramanik, S. Sreedharan, R. Tiwari, S. Dutta, N. Kandoth, S. Barman, S. O. Aderinto, S. Chattopadhyay, A. Das and J. A. Thomas, *Chem. Soc. Rev.*, 2022, **51**, 9882–9916.